

## Supporting Information

### Dual Modulation of Lattice Strain and Charge Polarization Induced by Co(OH)<sub>2</sub>/Ni(OH)<sub>2</sub> Interfaces for Efficient Oxygen Evolution Catalysis

Lin-Fei Gu, Cheng-Fei Li, Jia-Wei Zhao, Ling-Jie Xie, Jin-Qi Wu, Qian Ren and Gao-Ren Li\*

MOE Key Laboratory of Bioinorganic and Synthetic Chemistry, School of Chemistry, Sun Yat-Sen University,  
Guangzhou 510275, P.R. China

E-mail: [ligaoren@mail.sysu.edu.cn](mailto:ligaoren@mail.sysu.edu.cn)

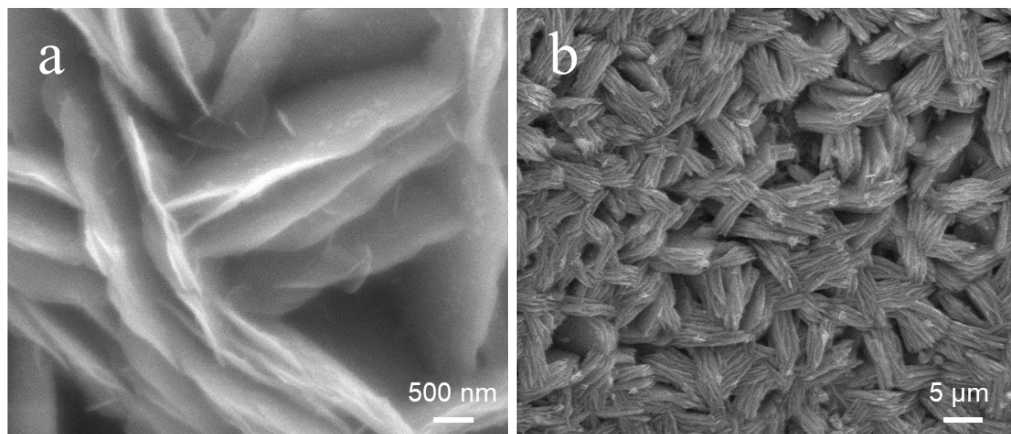


**Figure S1.** SEM images of Co(OH)<sub>2</sub> NSs@NF.

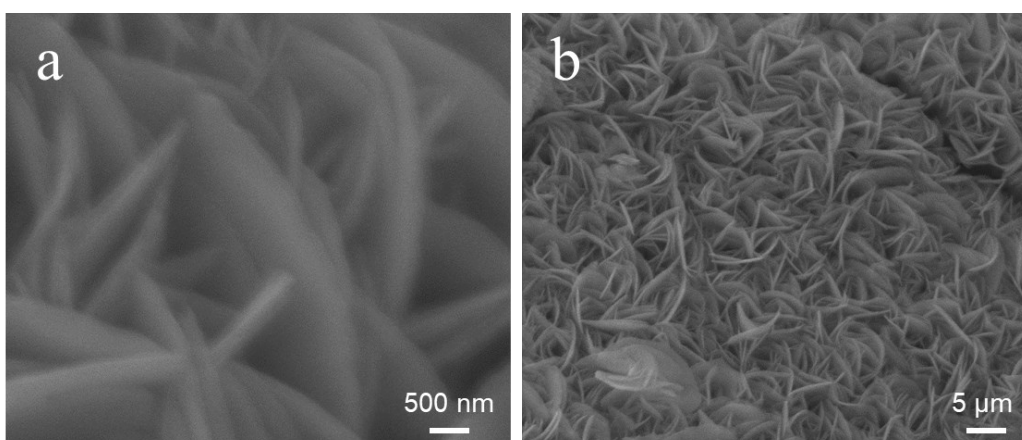


**Figure S2.** SEM images of Ni(OH)<sub>2</sub> NSs@NF.

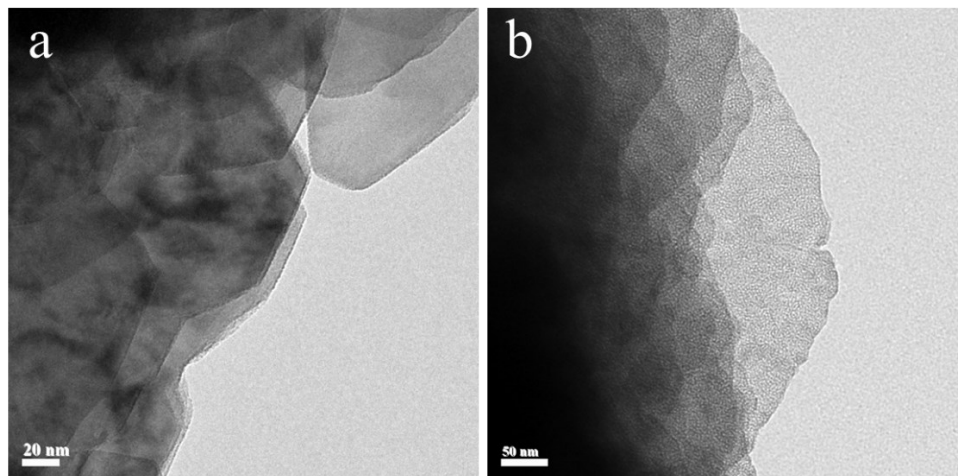


**Figure S3.** TEM images of Co(OH)<sub>2</sub> NSs@NF.

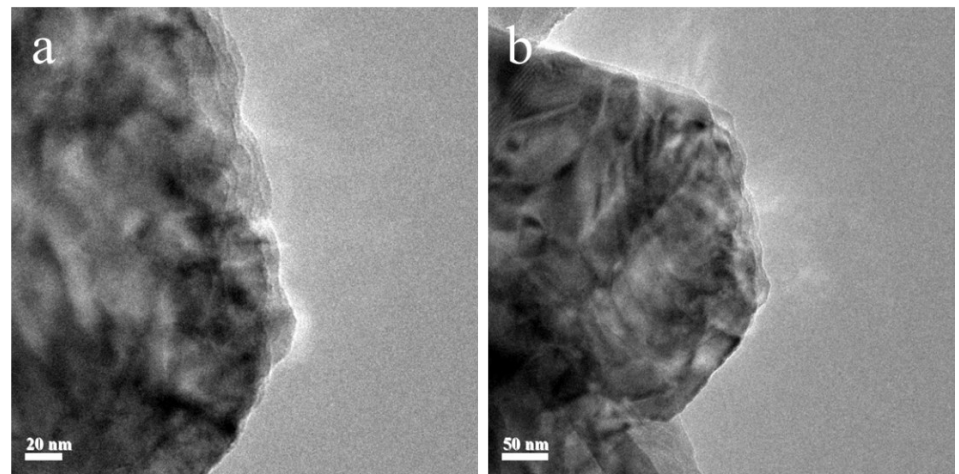


**Figure S4.** TEM images of Ni(OH)<sub>2</sub> NSs@NF.

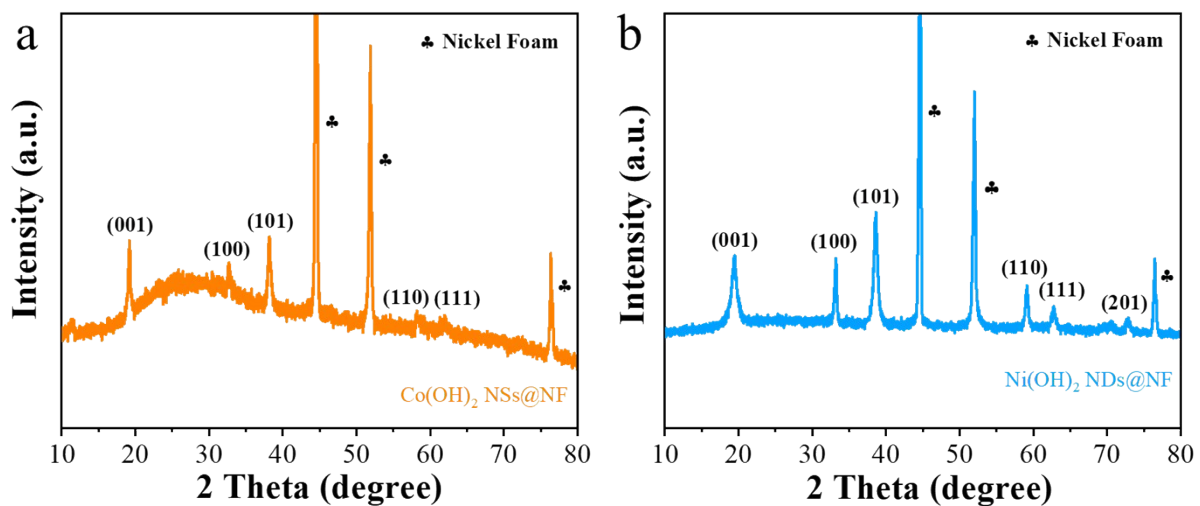


**Figure S5.** XRD patterns of (a)  $\text{Co}(\text{OH})_2$  NSs@NF and (b)  $\text{Ni}(\text{OH})_2$  NSs@NF.

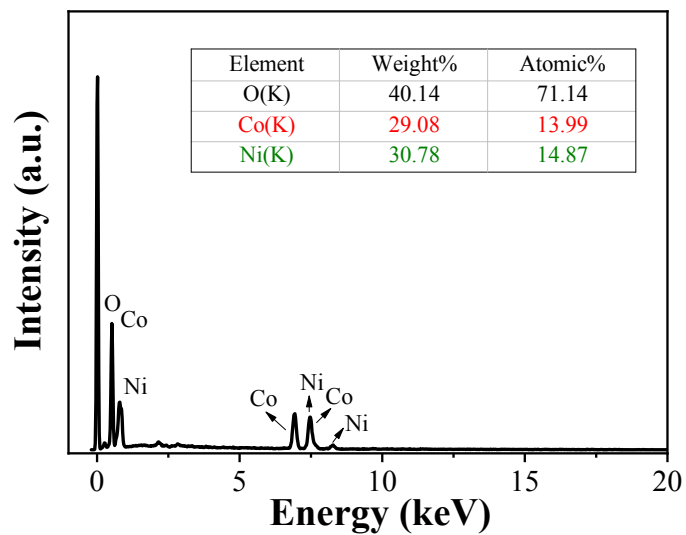


**Figure S6.** EDS spectrum of  $\text{Co}(\text{OH})_2/\text{Ni}(\text{OH})_2$  NSs (the sample is peeled off from the Nickel Foamed to reduce the influence of nickel in the substrate).

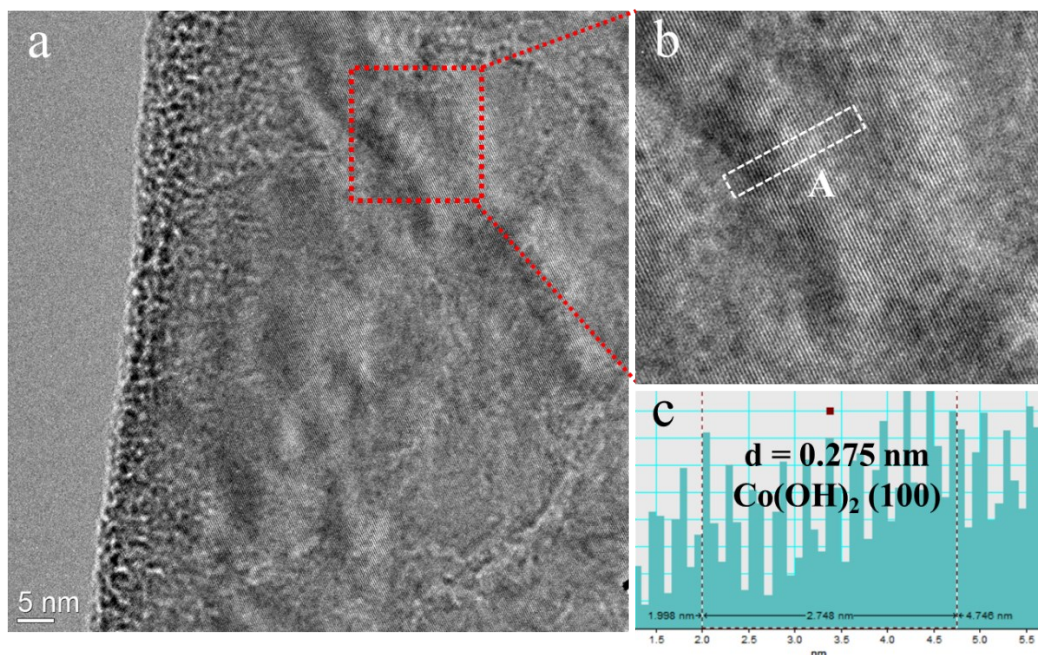


**Figure S7.** (a) HRTEM images and (b) its partial enlarged view of pure Co(OH)<sub>2</sub> nanosheets; (c) the line scans of the areas A in HRTEM image in (b) marked with white rectangles, which indicates a lattice fringe spacing of 0.275 nm, corresponding to Co(OH)<sub>2</sub> (100) (PDF#30-0443).

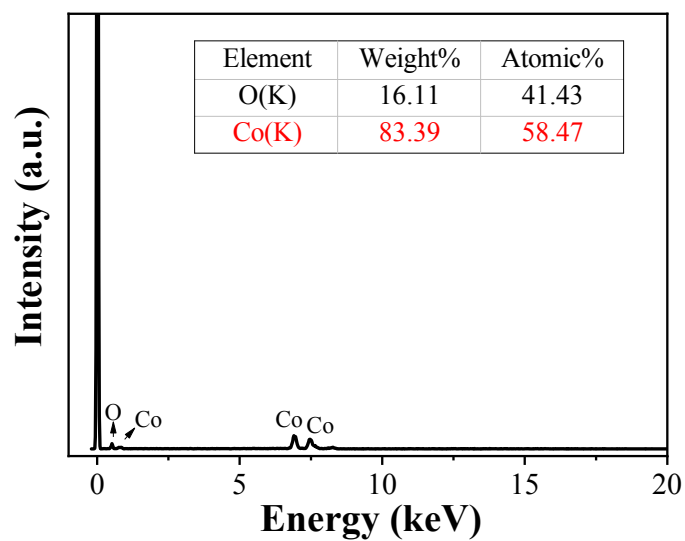


**Figure S8.** EDS spectrum of Co(OH)<sub>2</sub> NSs@NF.

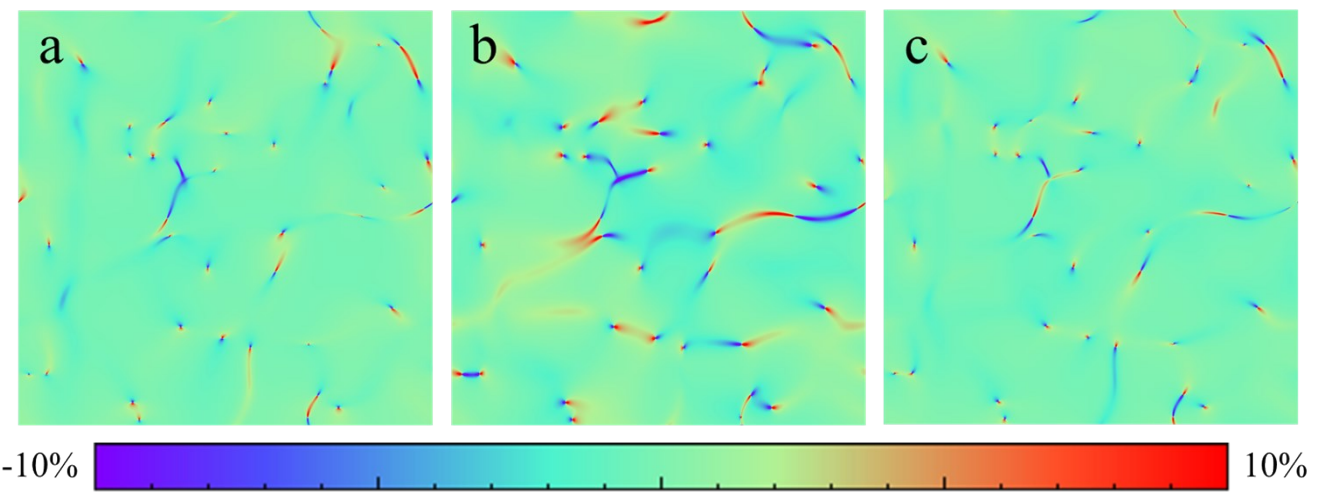


**Figure S9.** The strain tensor maps of (a) x direction ( $\epsilon_{xx}$ ), (b) y direction ( $\epsilon_{yy}$ ) and (c) xy shear ( $\epsilon_{xy}$ ) generated from the Figure S7a using geometric phase analysis.

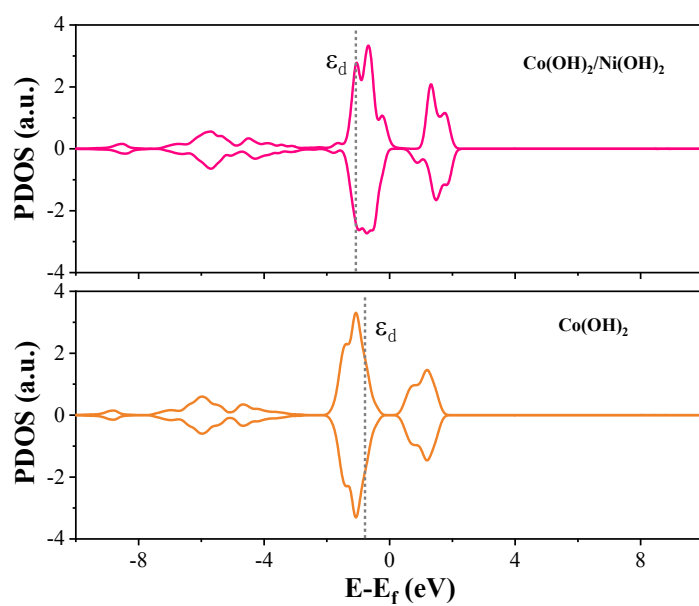


**Figure S10.** The projected density-of-states of Co d orbitals of  $\text{Co(OH)}_2/\text{Ni(OH)}_2$  and  $\text{Co(OH)}_2$ .

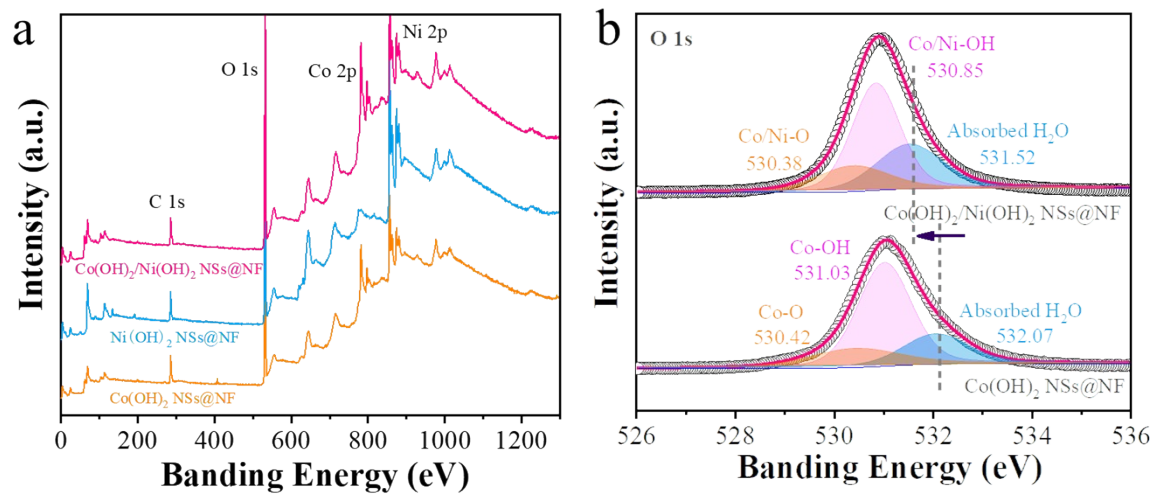


**Figure S11.** XPS spectra of (a) survey, (b) O 1s of Co(OH)<sub>2</sub> NSSs@NF, Ni(OH)<sub>2</sub> NSSs@NF and Co(OH)<sub>2</sub>/Ni(OH)<sub>2</sub> NSSs@NF.

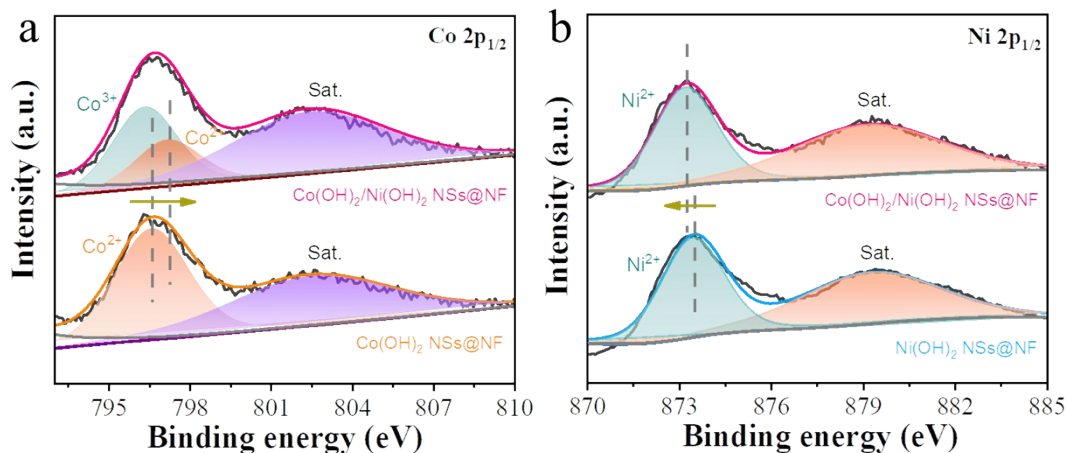


**Figure S12.** XPS spectra of (a) Co 2p<sub>1/2</sub>, (b) Ni 2p<sub>1/2</sub> for Co(OH)<sub>2</sub> NSSs@NF and Co(OH)<sub>2</sub>/Ni(OH)<sub>2</sub> NSSs@NF.

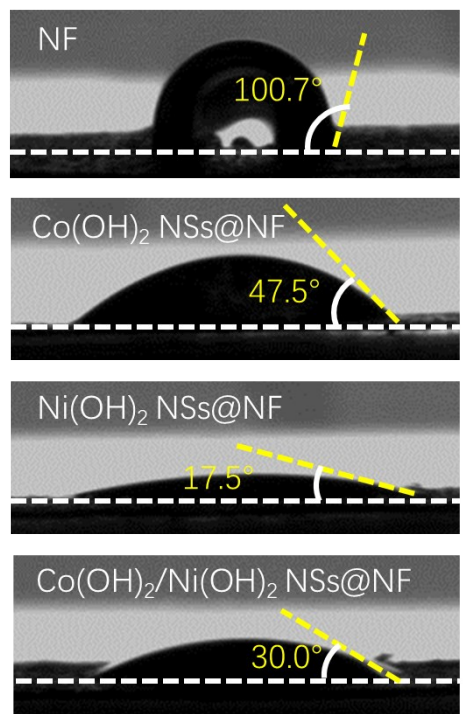


**Figure S13.** Contact angle measurements of samples NF, Co(OH)<sub>2</sub> NSs@NF, Ni(OH)<sub>2</sub> NSs@NF and Co(OH)<sub>2</sub>/Ni(OH)<sub>2</sub> NSs@NF.

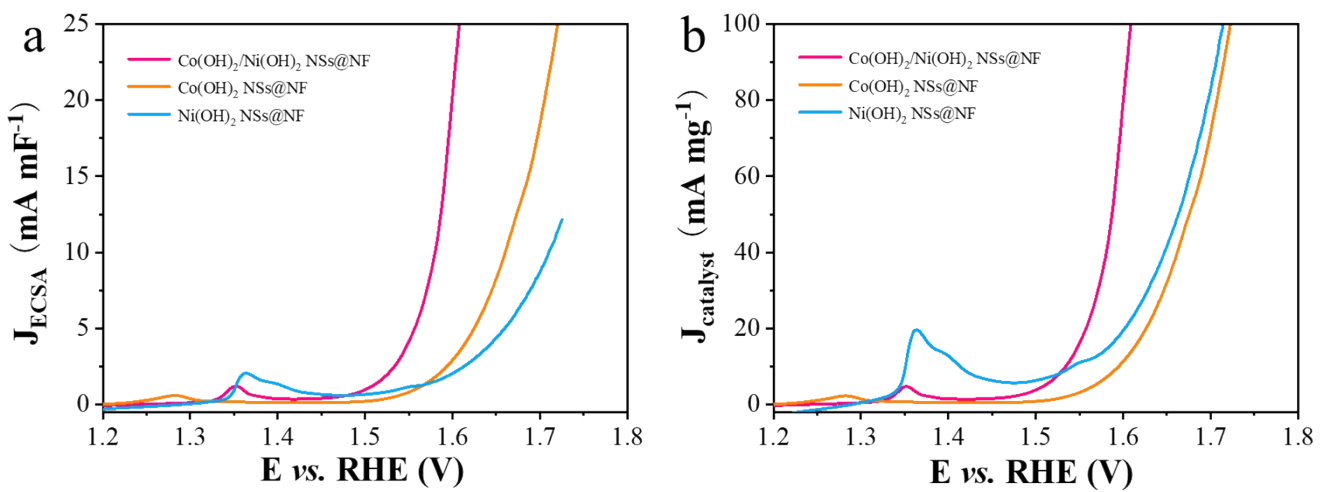


**Figure S14.** The OER polarization curves of  $\text{Co(OH)}_2/\text{Ni(OH)}_2$  NSs@NF,  $\text{Co(OH)}_2$  NSs@NF, and  $\text{Ni(OH)}_2$  NSs@NF in Figure 5(a) normalized by (a) electrochemically active area (ECSA) and (b) the loading mass of catalyst.

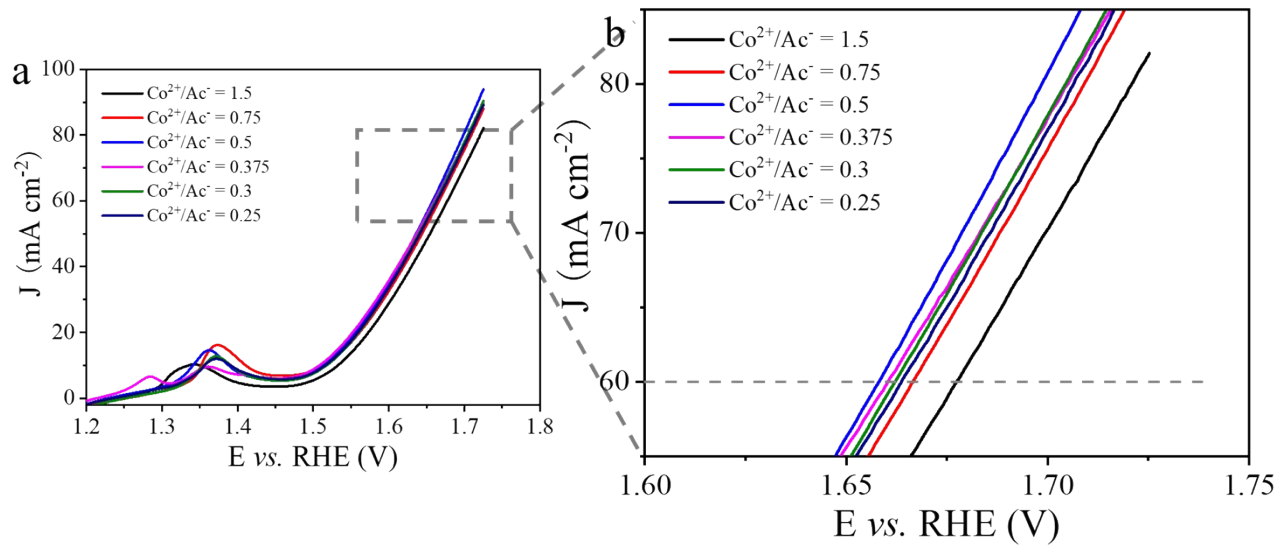


**Figure S15.** (a) OER polarization curves of  $\text{Co(OH)}_2/\text{Ni(OH)}_2$  NSs@NF based on different ratios of  $\text{Co}^{2+}/\text{Ac}^-$  ( $\text{Ac}^-$  represents acetate), (b) the partial enlarged view of (a) at  $60 \text{ mA cm}^{-2}$ .

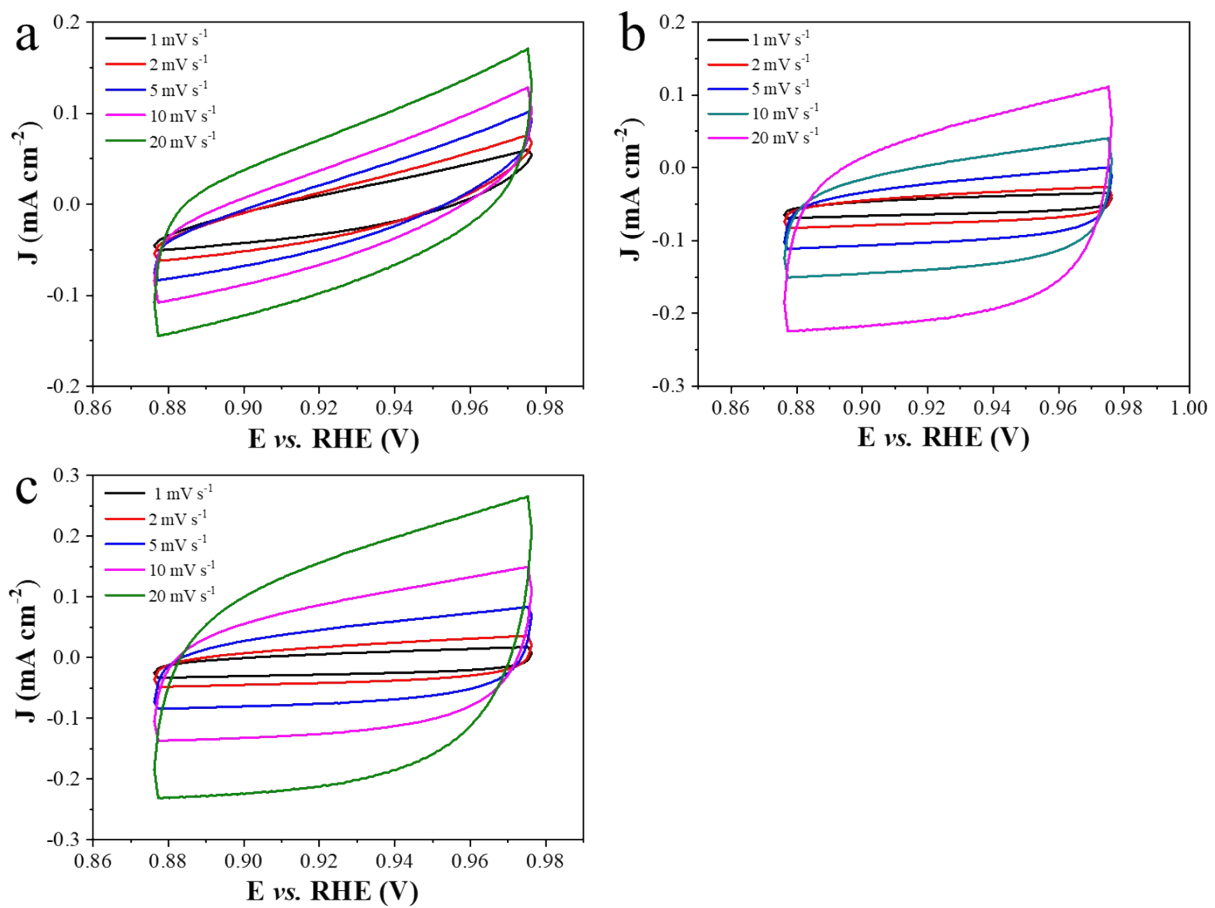


**Figure S16.** CVs of (a)  $\text{Ni(OH)}_2$  NSs@NF, (b)  $\text{Co(OH)}_2$  NSs@NF, (c)  $\text{Co(OH)}_2/\text{Ni(OH)}_2$  NSs@NF in the range of  $0.88 \sim 0.98$  V vs. RHE, measured in 1.0 M KOH solution, respectively.

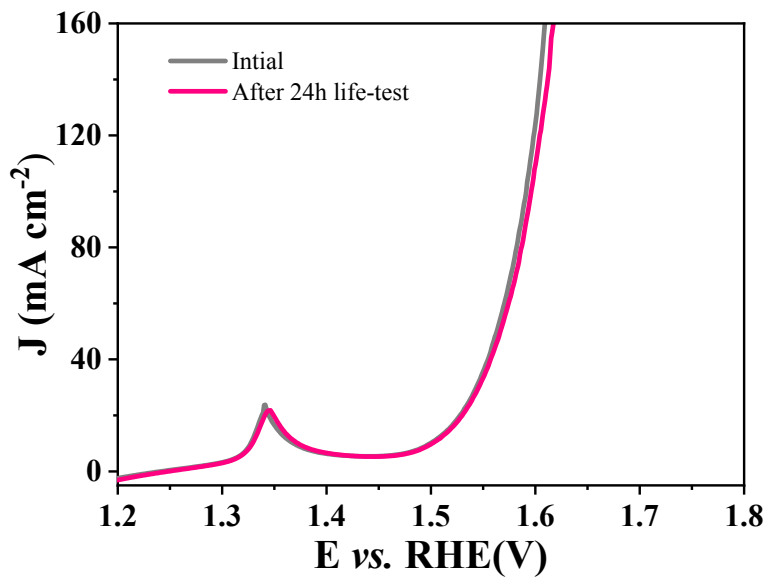


**Figure S17.** Polarization curves of before and after 24 h durability test at  $20 \text{ mA cm}^{-2}$  for  $\text{Co(OH)}_2/\text{Ni(OH)}_2$  NSS@NF.

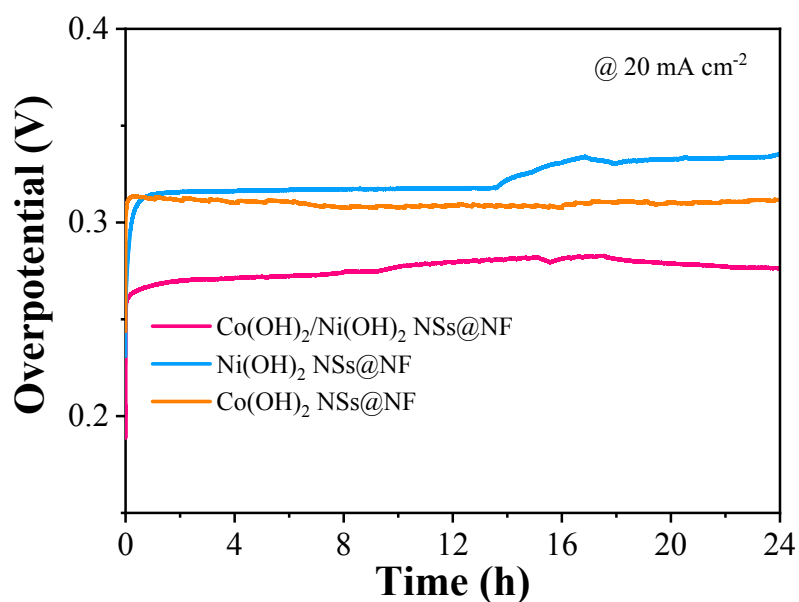


**Figure S18.** Galvanostatic measurements of  $\text{Co(OH)}_2/\text{Ni(OH)}_2$  NSS@NF,  $\text{Co(OH)}_2$  NSS@NF and  $\text{Ni(OH)}_2$  NSS@NF

at the current density of  $20 \text{ mA cm}^{-2}$ .

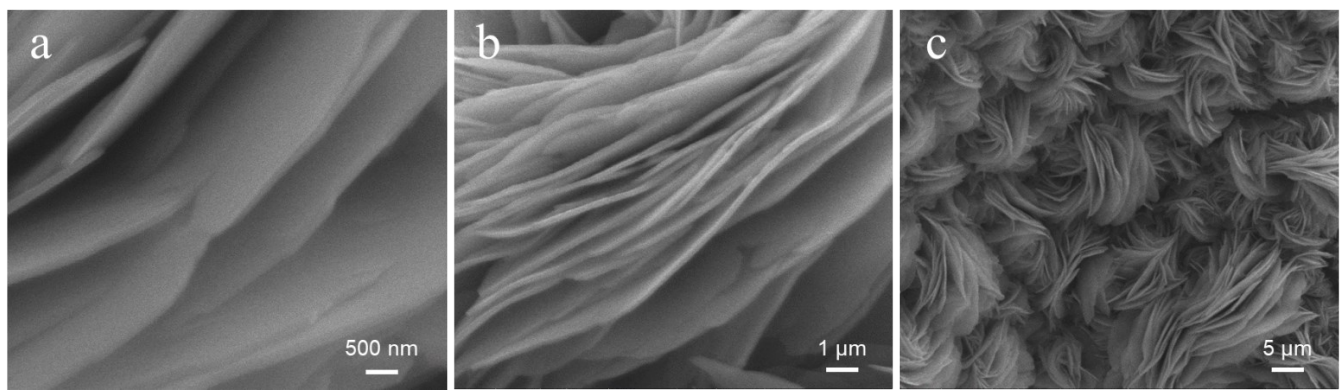


**Figure S19.** SEM images with different magnifications of  $\text{Co}(\text{OH})_2/\text{Ni}(\text{OH})_2$  NSs@NF after OER at  $20 \text{ mA cm}^{-2}$  for 24 h.

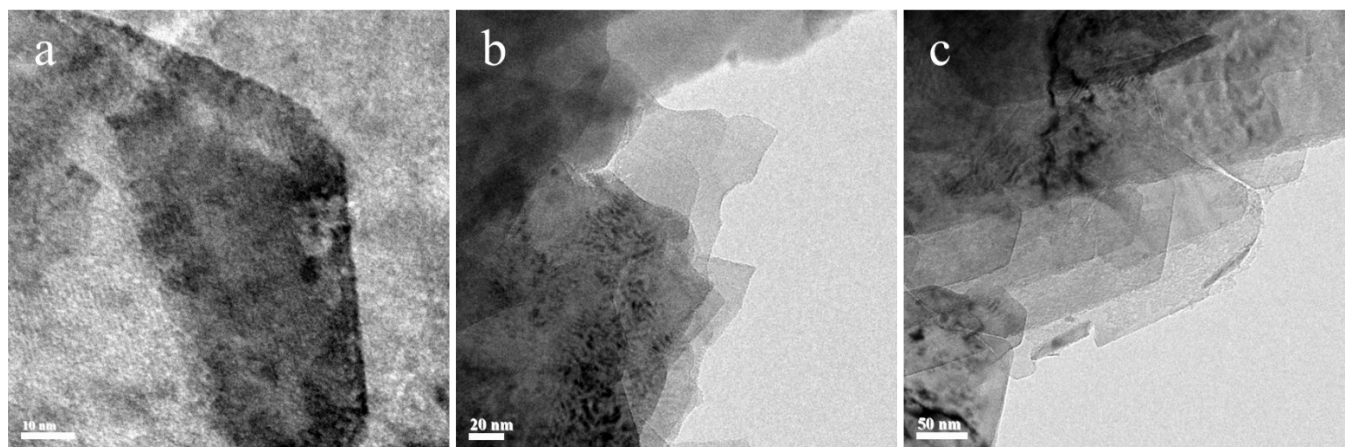


**Figure S20.** TEM images with different magnifications of  $\text{Co}(\text{OH})_2/\text{Ni}(\text{OH})_2$  NSs@NF after OER at  $20 \text{ mA cm}^{-2}$  for 24 h.

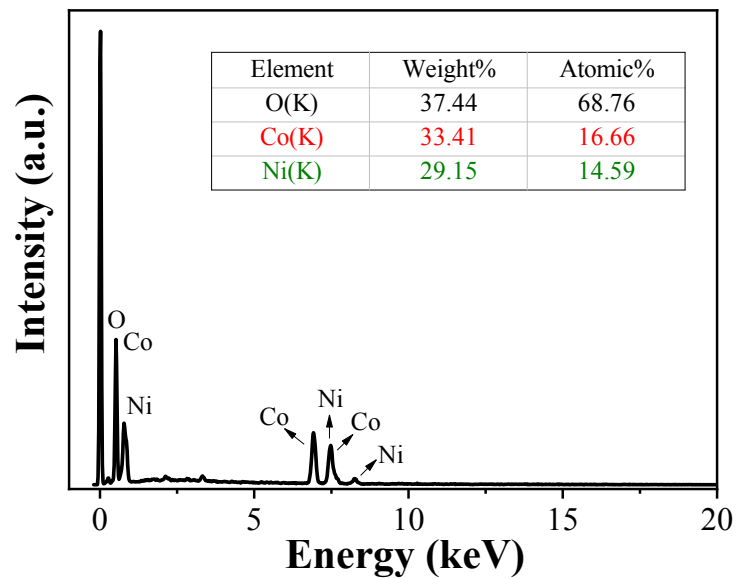


**Figure S21.** EDS spectrum of  $\text{Co}(\text{OH})_2/\text{Ni}(\text{OH})_2$  NSs after OER at  $20 \text{ mA cm}^{-2}$  for 24 h.

**Table S1.** Comparisons of representative cobalt-based and nickel-based OER electrocatalysts in alkaline electrolyte (1.0 M KOH solution).

Catalysts	$\eta@J$ (mV@mA cm <sup>-2</sup> )	Tafel slope (mV dec <sup>-1</sup> )	Reference
Co(OH) <sub>2</sub> /Ni(OH) <sub>2</sub> NSs	270@20	78	This work
NiCo LDHs	367@10	40	<i>Nano Lett.</i> <b>2015</b> , 15, 1421
NiCoP/C nanoboxes	330@10	96	<i>Angew. Chem. Int. Ed.</i> <b>2017</b> , 129, 3955
NiCo@NiCoO <sub>2</sub> /C PMRAs	366@20	84	<i>Adv. Mater.</i> <b>2018</b> , 30, 1705442.
Mo-NiCo <sub>2</sub> O <sub>4</sub> /Co <sub>5.47</sub> N/NF	310@50	55	<i>Small.</i> <b>2020</b> , 16, 1906775
NiCo <sub>2</sub> O <sub>4</sub> /CoMoO <sub>4</sub> /NF	390@50	102	<i>J. Mater. Chem. A.</i> <b>2018</b> , 6, 16950.
Co <sub>3</sub> O <sub>4</sub> /NiCo <sub>2</sub> O <sub>4</sub>	340@10	88	<i>J. Am. Chem. Soc.</i> <b>2015</b> , 137, 5590
NiO/Co <sub>3</sub> O <sub>4</sub> microcubes	290@10	73	<i>Chem. Commun.</i> <b>2019</b> , 55, 6515
NiCo <sub>2</sub> O <sub>4</sub> /CNTs	503@10	67	<i>J. Mater. Chem. A.</i> <b>2018</b> , 6, 7420
Co <sub>4</sub> Ni <sub>1</sub> -P	390@50	64	<i>Adv. Funct. Mater.</i> <b>2017</b> , 27, 1703455.
CoNi-S/NS-rGO-550	290@10	80	<i>ACS Appl. Mater. Interfaces.</i> <b>2020</b> , 12, 40186

$\eta$ : Overpotential (mV);

$J$ : Current density (mA cm<sup>-2</sup>);

PMRAs: Porous microrod arrays;

NF: Nickel foam;

CNTs: Carbon nanotubes;

rGO: Reduced graphene oxide.